Sequential growth of two-dimensional $MoSe_2$-WSe_2 lateral heterojunctions

Cite as: AIP Conference Proceedings **2265**, 030699 (2020); https://doi.org/10.1063/5.0018023
Published Online: 05 November 2020

Sharad Kumar Yadav, Vishal V. R. Nandigana, and Pramoda K. Nayak

Sequential Growth of Two-dimensional $MoSe_2$-WSe_2 Lateral Heterojunctions

Sharad Kumar Yadav [a,b)], Vishal V. R. Nandigana [b)], and Pramoda K. Nayak [a*)]

[a]*Department of Mechanical Engineering, Indian Institute of Technology Madras, Chennai, India 600036*
[b]*Department of Physics, Indian Institute of Technology Madras, Chennai, India 600036*

*)Corresponding author: pnayak@iitm.ac.in

Abstract. The two-dimensional (2D) heterojunctions of layered transition metal dichalcogenides (TMDs) with different bandgaps are the basis of modern electronic and optoelectronic devices such as high-speed transistors, light-emitting diodes, diode lasers and so on. Although, complex heterostructures (HSs) have been widely fabricated in the vertical direction via van der Waals (vdWs) stacking of different TMDs, but, atomic stitching of such 2D materials in the horizontal direction is proven to be so far most challenging. Here, we report a two-step sequential growth of monolayer n-type $MoSe_2$ - p-type WSe_2 lateral junction using chemical vapor deposition (CVD), which was confirmed from Raman and photoluminescence measurements. This work could be extended to other families of TMDs and provide a platform for the development of new device functionalities such as in-plane transistors and diodes to be integrated within a single atomically thin layer.

INTRODUCTION:

The 2D layered materials are gaining enormous attention among the research community in the past few years[1]. Graphene is the most studied 2D material, which exhibits remarkable electrical, mechanical and chemical properties and shown application in several areas such as photodetectors[2], light-emitting diode[3], high-speed transistor[4], and sensors[5]. However, the zero bandgaps of grapheme hinder its supremacy, particularly in digital electronics and optoelectronics[6]. Besides graphene, a range of other 2D material like hBN[7], Silicene, Phosphene, TMDs, etc[8] got attention since last decade. Among all, the monolayer semiconducting TMDs with chemical formula MX_2 (M=Mo, W, and so on; X=S, Se, or Te) are very interesting as they offer direct bandgap in the technologically important spectral range 1-3 eV and hence is suitable for the optoelectronic and photonic applications. These TMD monolayers could be combined to create either vdW heterostructures by stacking layer by layer[9] or stitched together in-plane to form lateral heterostructures (LHS)[10]. The above HSs would enable band engineering within the 2D plane and open up new realms in device physics and engineering.[11] In recent years several vdW HSs including MoS_2-$MoSe_2$[12], WS_2-WSe_2[12], $MoSe_2$-WSe_2[13],WS_2-MoS_2[14] has been reported, in which most of the HSs are formed by physical transfer method[15].The physical transfer method includes miss-orientation and contamination issues at the interface/junction[10], [16]. However, the growth of LHS is in the nascent stage as it is very challenging. It is reported that using CVD, LHS with a smooth, sharp and noncontaminated interface can be formed.[14]

The growth of LHS is possible either by one step (in-situ) process[9][14] or by two-step process[14] using CVD. Each of them has its own advantage and limitation. In one step process, all the solid precursors are kept together in the chamber to vaporize and deposit on to the substrate. while in the two-step CVD process, sequentially one material is deposited first and then followed the second. During one step deposition method, the deposited junction region contains an alloy structure since all the precursor presents together in the vapor phase during deposition. Hence the interfacial region of LHS may end up with either with different transition metal or with different chalcogen[6], which hinders in achieving the desired clean interfacial LHS. On the contrary, the two-step CVD

DAE Solid State Physics Symposium 2019
AIP Conf. Proc. 2265, 030699-1–030699-4; https://doi.org/10.1063/5.0018023
Published by AIP Publishing. 978-0-7354-2025-0/$30.00

process has a lower tendency to get alloy structure at the junction since one precursor is deposited at a time. The challenge with the two-step CVD process is during the change of precursor, the surrounding environment may introduce some contamination on the deposited interface. In the present work, we have carried out two-step sequential growth of monolayer n type $MoSe_2$-p type WSe_2 lateral junction with a very clean interface using CVD.

EXPERIMENTAL METHODS

CVD synthesis of monolayer $MoSe_2$:

The monolayer $MoSe_2$ crystal was grown using atmospheric pressure chemical vapor deposition (APCVD) system **(Figure 1a)**. A (~2x1 cm^2) sapphire substrate was cut form wafer and cleaned with acetone, IPA, and DI water. The two source material MoO_3 (60 mg) and Se (100 mg) were taken in the ceramic crucible boat and placed in high-temperature and low-temperature zone respectively. These boats were kept in 2-inch diameter quartz tube inside the outer tube. The cleaned sapphire substrate was placed adjacent to MoO_3 source crucible as a deposition acceptor. In the first step, the temperature of MoO_3 powder was raised to 700^0 C (with 15^0 C/min rate) and then raised to 800^0 C within 7 minutes **(Figure 1b)**. The Se source powder temperature was raised to 300^0 C during this 7 minutes with the separate heating arrangement. In the second step, A constant temperature of 800^0 C in MoO_3 source zone and 300^0 C in Se source zone was maintained for 30 minutes **(Figure 1b)**. Ar (67 sccm) and H_2 (8 sccm) were used as a transport carrier for vaporized precursors and selenization respectively. After the deposition, the furnace was cooled down to room temperature in Ar atmosphere only.

CVD synthesis of monolayer WSe_2:

The monolayer WSe_2 crystal was grown using low-pressure CVD **(Figure 1a)**. The Ar carrier gas and selenizing H_2 gas flow rates were 60 sccm and 20 sccm, respectively. The WO_3 (50 mg) and Se (140 mg) were used as source precursors. The constant temperature of WO_3 was maintained at 870° C and of Se at260° C for 60 minutes **(Figure 2a)**. The pressure of the chamber was maintained at 15 Torr throughout the whole process.

$MoSe_2$-WSe_2 heterojunction fabrication:

The as-grown monolayer $MoSe_2$/sapphire flakes were placed in the low-pressure CVD system and WSe_2 deposition parameters were used as mentioned above to grow $MoSe_2$-WSe_2 in-plane heterostructures on sapphire substrates.

Raman and PL spectra measurements:

The Raman and PL spectra were carried out at room temperature on $MoSe_2$/WSe_2 HS flakes,prepared on sapphireand 488 nm laser (2.54 eV) were used as an excitation source, with the focused spot size <1μm on the sample and the spatial resolution was 1cm^{-1}(obtained with 1800 Grooves/mm grating). To avoid the local heating the laser power was kept at 50 μW.

RESULT AND DISCUSSION

Figure 1a and**1b** show the schematics of CVD set up and growth profile $MoSe_2$. The optical microscopic (OM) image of as-grown $MoSe_2$ crystals on sapphire is shown in (**Figure 1c)**. Most of the flakes are in a triangular shape and some in truncated shape. The Raman and PL measurements were carried out on the as-grown flakes and the spectra were plotted in **Figure 1d&1e**. The presence of out-of-plane mode A_{1g} at 244 cm^{-1} and in-plane mode E_{2g} at 294 cm^{-1} along with the absence of the layer number sensitive mode A_{2g} at 353 cm^{-1} of the characteristic Raman vibration mode confirmed the growth of monolayer $MoSe_2$ crystal. The growth of monolayer $MoSe_2$ crystal is further verified using PL spectra with the peak at 1.51eV**(Figure 1e)**[15].

Similarly, the schematic of the growth profile and OM images of as-grown WSe_2 crystals on sapphire are shown in **Figure 2a& 2b**. The crystals are in a triangular shape. The Raman spectra of a monolayer WSe_2 crystal is shown in **Figure 2c**. The presence of E'_{2g} at 250 cm^{-1} and A_{1g} at 262 cm^{-1} along with the absence of the layer number sensitive mode A_2'' at 309 cm^{-1} of the characteristic Raman vibration mode confirmed the growth of monolayer WSe_2 crystal. The growth of monolayer WSe_2 crystal is further verified using PL spectra with a peak at 1.63 eV **(Figure 2d)**.

As stated in the experimental section, the as-grown monolayer $MoSe_2$/sapphire flakes were placed in the APCVD system used for WSe_2 growth and the growth process was carried out using the WSe_2 deposition parameters. The sharp edges of $MoSe_2$ triangular flakes act as nucleation sites and WSe_2 try to grow from the edges to form $MoSe_2$-

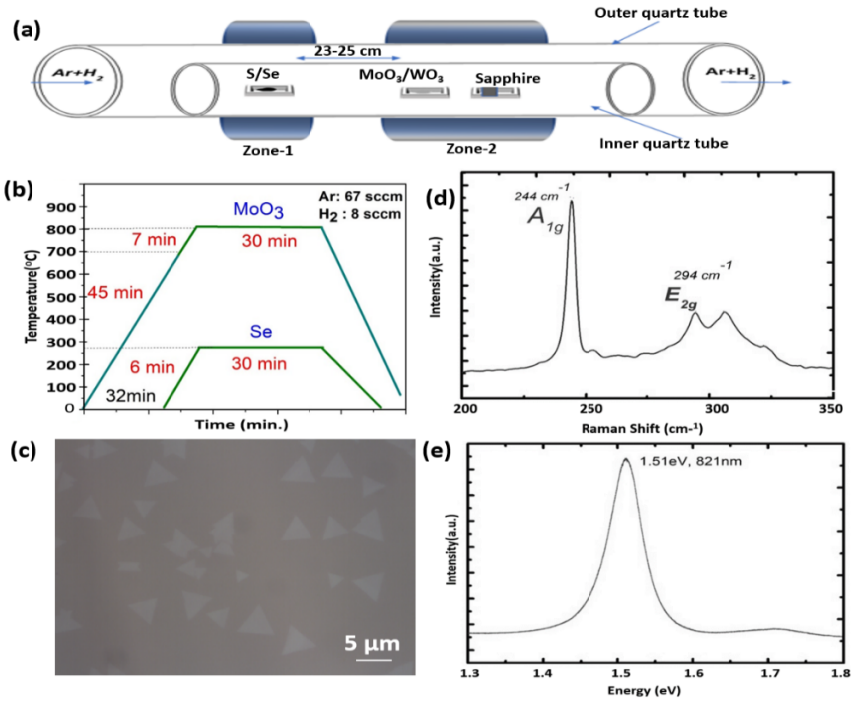

FIGURE 1. Growth process and characterization of monolayer $MoSe_2$. (a) Schematic of $MoSe_2$ and WSe_2 growth process using CVD. (b) The temperature profiles of precursor powders and gas flow rates. (c) OM image of as-prepared $MoSe_2$ flakes. (d,e) Raman spectrum and PL spectrum measured on a $MoSe_2$ flake.

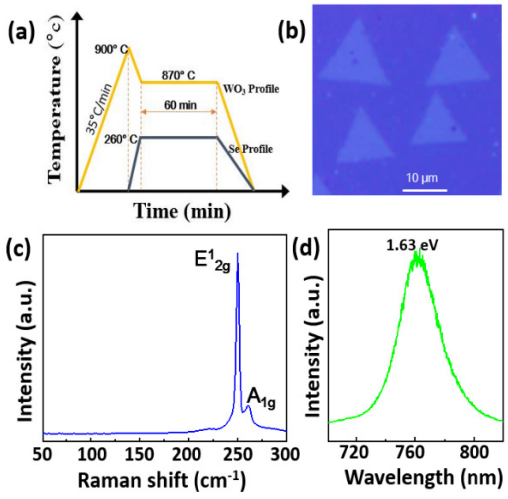

FIGURE 2. Growth process and characterization of monolayer WSe2. (a) The temperature profiles of the precursor powders displayed in the figure. (b) OM image of WSe2 grains on the sapphire substrate. (c,d) Raman spectrum and PL spectrum measured on a WSe_2 flake.

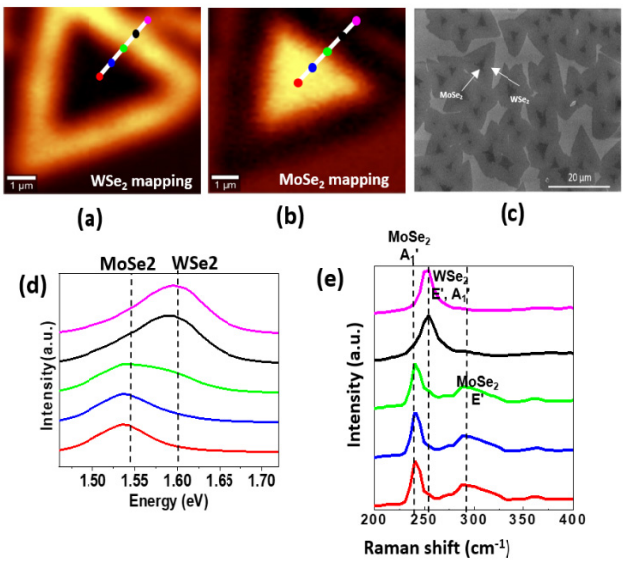

FIGURE 3. Characterization of LHS monolayer $MoSe_2$-WSe_2. (a) PL mapping of WSe_2 in LHS. (b) PL mapping of $MoSe_2$ in LHS (c) SEM image(d) The PL spectra and (e) Raman spectra extracted from the mapping points along the line.

WSe_2 LHS as shown in SEM images **(Figure 3c)** similar to *Huang et al.*[17]. The inner contrasts in the SEM image correspond to $MoSe_2$ and outer contrasts belong to WSe_2 **(Figure 3c)** In order to confirm the formation of LHS, Raman, and PL mapping were carried out on a selected LHS flake shown in **Figure3a** and **Figure3b** respectively. From the mapping, the corresponding PL spectra and Raman spectra (Raman mapping is done but not shown here) were extracted at different mapping points and plotted in **Figure3d** and **Figure3e,** respectively. The point mapping across the line clearly shows that there is a formation of $MoSe_2$-WSe_2 LHS with a sharp interface. Furthermore, there is no sign of nucleation of WSe_2 on top of the $MoSe_2$, implies no vertical HS formation.

CONCLUSION

In summary, we have successfully synthesized monolayer $MoSe_2$ and WSe_2 flakes using CVD. By following the same deposition parameters, we could able to achieve two-step sequential growth of n-type $MoSe_2$ - p-type WSe_2 lateral junction, which is confirmed from SEM, PL and Raman analysis. These lateral heterojunctions of monolayer n-type $MoSe_2$ - p-type WSe_2 provide a platform for the development of new device functionalities such as in-plane transistors and diodes to be integrated within a single atomically thin layer. The further optimization in a deposition is needed to scale-up such junction along with other combination of TMDs.

REFERENCES

1. G. R. Bhimanapati *et al.*, "Recent Advances in Two-Dimensional Materials beyond Graphene," *ACS Nano*, vol. 9, no. 12, pp. 11509–11539, Dec. 2015.
2. Z. Yin *et al.*, "Single-Layer MoS2 Phototransistors," *ACS Nano*, vol. 6, no. 1, pp. 74–80, Jan. 2012.
3. R. S. Sundaram *et al.*, "Electroluminescence in Single Layer MoS2," *Nano Lett.*, vol. 13, no. 4, pp. 1416–1421, Apr. 2013.
4. B. Radisavljevic and A. Kis, "Mobility engineering and a metal–insulator transition in monolayer MoS2," *Nat. Mater.*, vol. 12, p. 815, Jun. 2013.
5. F. K. Perkins, A. L. Friedman, E. Cobas, P. M. Campbell, G. G. Jernigan, and B. T. Jonker, "Chemical Vapor Sensing with Monolayer MoS2," *Nano Lett.*, vol. 13, no. 2, pp. 668–673, Feb. 2013.
6. E. Gibney, "The super materials that could trump graphene," *Nature*, vol. 522, no. 7556, pp. 274–276, 2015.
7. K. Zhang, Y. Feng, F. Wang, Z. Yang, and J. Wang, "Two dimensional hexagonal boron nitride (2D-hBN): synthesis, properties and applications," *J. Mater. Chem. C*, vol. 5, no. 46, pp. 11992–12022, 2017.
8. S. Balendhran, S. Walia, H. Nili, S. Sriram, and M. Bhaskaran, "Elemental Analogues of Graphene: Silicene, Germanene, Stanene, and Phosphorene," *Small*, vol. 11, no. 6, pp. 640–652, Feb. 2015.
9. K. Kang *et al.*, "Layer-by-layer assembly of two-dimensional materials into wafer-scale heterostructures," *Nature*, vol. 550, p. 229, Sep. 2017.
10. Y. Gong *et al.*, "Vertical and in-plane heterostructures from WS2/MoS2 monolayers," *Nat. Mater.*, vol. 13, p. 1135, Sep. 2014.
11. Y. Liu, S. Zhang, J. He, Z. M. Wang, and Z. Liu, "Recent Progress in the Fabrication, Properties, and Devices of Heterostructures Based on 2D Materials," *Nano-Micro Lett.*, vol. 11, no. 1, p. 13, 2019.
12. X. Duan *et al.*, "Lateral epitaxial growth of two-dimensional layered semiconductor heterojunctions," *Nat. Nanotechnol.*, vol. 9, p. 1024, Sep. 2014.
13. P. K. Nayak *et al.*, "Probing Evolution of Twist-Angle-Dependent Interlayer Excitons in MoSe2/WSe2 van der Waals Heterostructures," *ACS Nano*, vol. 11, no. 4, pp. 4041–4050, Apr. 2017.
14. Y. Gong *et al.*, "Two-Step Growth of Two-Dimensional WSe2/MoSe2 Heterostructures," *Nano Lett.*, vol. 15, no. 9, pp. 6135–6141, Sep. 2015.
15. X. Wang *et al.*, "Chemical Vapor Deposition Growth of Crystalline Monolayer MoSe2," *ACS Nano*, vol. 8, no. 5, pp. 5125–5131, May 2014.
16. Z. Liu *et al.*, "In-plane heterostructures of graphene and hexagonal boron nitride with controlled domain sizes," *Nat. Nanotechnol.*, vol. 8, p. 119, Jan. 2013.
17. C. Huang *et al.*, "Lateral heterojunctions within monolayer MoSe2–WSe2 semiconductors," *Nat. Mater.*, vol. 13, p. 1096, Aug. 2014.